21st Australasian Fluid Mechanics Conference
Adelaide, Australia
10-13 December 2018

Compression Wave Propagation in Asymmetrical Canals

R. Fernando[1], X. Leng[1] and H. Chanson[1]

[1]The University of Queensland
School of Civil Engineering, Brisbane 4072, Australia

Abstract

In an open channel, a compression wave is the unsteady flow motion induced by a sudden rise in water elevation. It may include rejection surges in hydro-power canals and surges induced by rapid gate operation. The present investigation considered the upstream propagation of positive surges in an asymmetrical trapezoidal channel with a 1:3 transverse slope. Detailed experiments were performed in a 19 m long 0.7 m wide flume. Unsteady measurements were conducted using acoustic displacement meters, ADV velocimeter and ADV Profiler. Unsteady experiments were repeated 25 times and the results were ensemble-averaged. A key feature was the three-dimensional unsteady flow motion, yielding complicated transient secondary motion.

Introduction

In an open channel, a compression wave is a very-unsteady rapidly-varied flow motion characterised by a sudden rise in water surface elevation (Stoker 1957). Also called a positive surge and translating hydraulic jump, a compression wave can travel over very long distance because it can absorb random disturbances on both sides of the surge, making the compression wave stable and self-perpetuating (Henderson 1966, Chanson 2004). Man-made applications include rejection and load acceptance surges in hydropower canals following rapid turbine start or stoppage, as well as surges in water supply channels during rapid gate operation (Jaeger 1956). Related analogies include supernova explosion, black hole theory and Hawking effect (Foglizzo et al. 2015, Berry 2018). While simple one-dimensional modelling may be successfully applied, the approach does not provide any information on the unsteady turbulence and three-dimensional hydrodynamic transient flows. As an illustration, the Oraison hydropower canal in the Durance Valley, France, experienced operational incidents in the 1960s. Extensive field, laboratory and numerical investigations were conducted in the 1960s (Cunge 1966, Ponsy and Carbonnell 1966, Preissman and Cunge 1967) and the results led to operational restrictions, because of a lack of understanding of the local turbulent processes.

Most investigations of compression waves were conducted in rectangular flumes, except for limited free-surface observations in trapezoidal channels (e.g. Sandover and Taylor 1962, Benet and Cunge 1971, Treske 1994) and a recent study in an asymmetrical channel (Kiri et al. 2018). In the present study, detailed free-surface and velocity measurements were performed in a large-size flume with asymmetrical shape, the focus being the transient turbulence characteristics of the three-dimensional compression wave motion.

Methods, Facility and Instrumentation

Physical modelling was undertaken based upon a Froude similarity in a 19 m long 0.7 m wide horizontal channel, previously used by Leng and Chanson (2016,2017) with a rectangular cross-section, and Kiri et al. (2018) with a 1V:5H transverse bed slope. The present bed configuration included a 0.280 m wide horizontal section besides a 0.42 m wide 1V:3H sideslope made out of PVC (Fig. 1a). A fast-closing gate was located at the downstream end of the flume, with its rapid closure inducing a compression wave propagating upstream. Figures 1b and 1c illustrate the upstream propagation of compression wave.

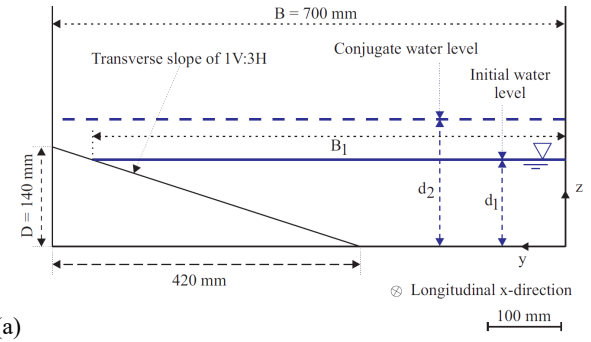

(a)

(b)

(c)

Figure 1. Compression wave propagation in an asymmetrical trapezoidal channel. (a) Un-distorted definition sketch. (b) Looking downstream for Q = 0.026 m^3/s, Fr_1 = 1.45. (c) Looking downstream for Q = 0.054 m^3/s, Fr_1 = 1.4, with dye injection.

The discharge was supplied through an upstream intake equipped with baffles, flow straighteners and a three-dimensional convergence delivering smooth inflow conditions. The flow rate was recorded with a magneto flow meter. In steady flows, the water depths were measured using rail mounted pointer gauges and the velocity measurements were conducted with a Dwyer® 166 Series Prandtl-Pitot tube (∅ = 3.18 mm). The Prandtl-Pitot tube was calibrated to provide the boundary shear stress with the tube lying on the boundary (Cabonce et al 2018). The unsteady water depths were recorded non-intrusively using a series of acoustic displacement meters Microsonic™ Mic+ located above the water surface (Fig. 1c). The sensors were calibrated against

the pointer gauge in steady flows. Unsteady velocity measurements were conducted with an acoustic Doppler velocimeter (ADV) Profiler Nortek^{TM} Vectrino II equipped with a three-dimensional down-looking head, and with an ADV Nortek^{TM} Vectrino + equipped with a three-dimensional side-looking head. The ADV Profiler was sampled at 100 Hz and the ADV Vectrino+ at 200 Hz. Both systems were located at a distance x = 8.6 m downstream of the canal's upstream end. The experiments were documented using a digital SLR camera Pentax^{TM} K-3 as well as a digital camera Casio^{TM} Exilim EX-10 with high-speed video capabilities.

Steady flow observations were conducted for discharges ranging from 0.006 m^3/s to 0.10 m^3/s. The open channel flow was at uniform equilibrium along most of the flume length and the flow motion was subcritical. The free-surface was horizontal in the transverse direction. All results showed a faster flow towards the deeper section of the channel (Fig. 2).

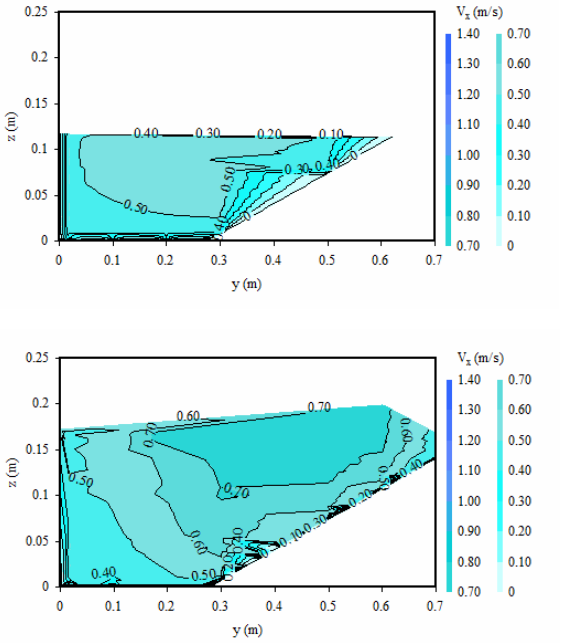

(a)

(b)

Figure 2. Longitudinal velocity contour maps in steady flows in asymmetrical canal. Flow conditions: (a) Q = 0.026 m^3/s, d = 0.117 m, x = 8.6 m. (b) Q = 0.054 m^3/s, d = 0.17 m, x = 8.6 m.

In steady flows, the boundary shear stress distribution was not uniform along the wetted perimeter. Large variations were observed along both the sidewalls and inclined bed. Minimum boundary shear stress was observed at the corners. Experimental results are shown in Figure 3, where the vertical solid line corresponds to the bottom right corner (y=0, z-0), and the vertical dashed lines represent the edges of the inclined transverse slope.

For all unsteady experiments, the compression waves were generated by the fast closure of the downstream gate and the surge propagated upstream against the initially-steady flow. Figure 1b and 1c show photographs of advancing compression waves. The gate closure time was between 0.1 s and 0.2 s, small enough to have no discernible effect on the compression wave propagation. The surge strength, defined by its Froude number, could be decreased by increasing the downstream gate opening h after closure for a given initial discharge. Detailed unsteady free-surface and velocity measurements were conducted at x = 8.6 m. Table 1 summarises the experimental flow conditions, where Q is the initial steady water discharge, d_1 is the initial water depth (Fig. 1a), and Fr_1 and Re_1 are the compression wave Froude and Reynolds numbers defined for a non-rectangular channel as:

$$Fr_1 = \frac{V_1 + U}{\sqrt{g \frac{A_1}{B_1}}} \quad (1)$$

$$Re_1 = \rho \frac{(V_1 + U)\frac{A_1}{B_1}}{\mu} \quad (2)$$

with V_1 the initial flow velocity, U the wave celerity positive upstream, g the gravity acceleration, A_1 and B_1 the initial flow cross-section area and free-surface width respectively, and ρ the water density and μ the water dynamic viscosity.

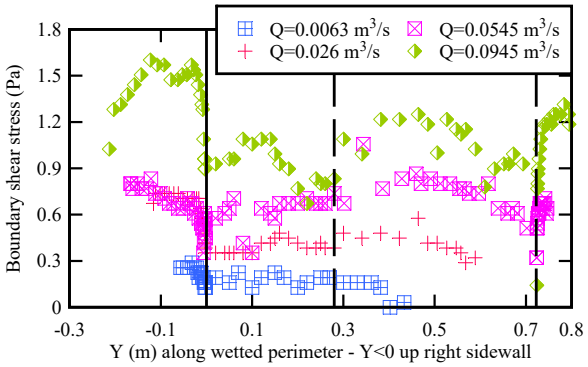

Figure 3. Transverse distributions of boundary shear stress in steady flows in asymmetrical canal. Y = 0 at bottom left corner of channel.

Q (m^3/s)	d_1 (m)	h (m)	U (m/s)	Fr_1	Re_1
0.026	0.106	0	0.67	1.41	0.95×10^5
		0.010	0.66	1.44	0.94×10^5
		0.015	0.61	1.38	0.90×10^5
		0.025	0.5	1.21	0.82×10^5
0.054	0.151	0	0.85	1.47	1.7×10^5
		0.015	0.77	1.46	1.6×10^5
		0.030	0.72	1.37	1.5×10^5
		0.050	0.52	1.21	1.3×10^5
0.094	0.195	0	1.1	1.56	3.0×10^5
		0.015	1.06	1.54	3.0×10^5
		0.030	0.90	1.44	2.8×10^5
		0.065	0.85	1.37	2.7×10^5

Table 1. Experimental investigations of compression waves in asymmetrical canals.

Basic unsteady flow observations

Visual and video observations were performed for a range of initial flow conditions, with initial depths d_1 measured next to the right sidewall (Table 1). Figures 1b and 1c show two pictures. For all conditions, several compression wave flow patterns were observed at x = 8.6 m, depending upon the surge Froude number Fr_1 and relative initial flow depth d_1/D with D the maximum height of the transverse bed slope (D = 0.140 m, Fig. 1a). For $d_1/D < 1$, the initial free-surface width B_1 was less than the full canal width B = 0.70 m. When the compression wave advanced, it expanded over the transverse slope as illustrated in Figures 1a and 1b, and the conjugate free-surface width was greater than the initial one. For $d_1 > D$, the initial and conjugate free-surface widths were identical, as seen in Figure 1c. In all cases, a key feature was the three-dimensional shape of the bore. Within the experimental flow conditions (Table 1), the compression wave was breaking in

shallow water next to the left sidewall, while strong secondary waves followed the wave front in deep waters towards the right sidewall (Fig. 1c). Further the leading edge of the compression wave passed first the sampling location in the shallow water section. The compression wave front propagated upstream with an angle to the left sidewall less than 90°, as seen in Figures 1b and 1c, although the celerity of the surge was the same across the canal. Note that, in the present study, the compression wave surface rose above the end of the transverse slope and the conjugate free-surface width was B_2 = B = 0.70 m. Free-surface measurements showed the three-dimensional nature of the compression waves. Figure 4 shows typical ensemble-averaged free-surface data at two transverse locations y. The experiments were repeated 25 times and ensemble-averaged in terms of the median surface elevation.

The present observations showed similarities with compression wave observations in a compound flume (Pan and Chanson 2015) and in an asymmetrical canal (Kiri et al. 2018), as well as with field observations of tidal bores in natural channels, as in the Garonne River (Chanson et al. 2011, Keevil et al. 2015, Reungoat et al. 2017).

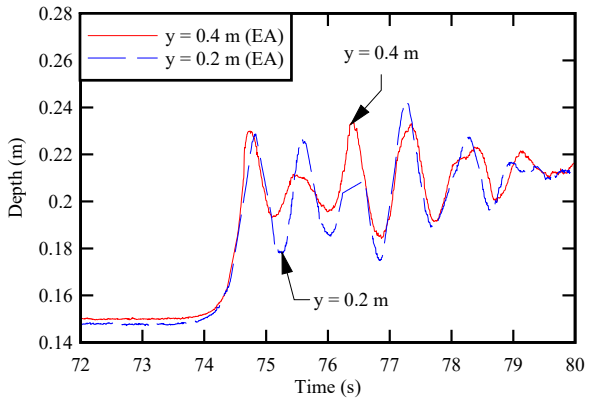

Figure 4. Time-variations of ensemble-median water surface for Fr_1 = 1.46, d_1 = 0.151 m, Re_1 = 1.6×10^5 at x = 8.6 m and two transverse locations: y = 0.2 m and 0.4 m.

Unsteady free-surface and velocity measurements

The compression waves were generated at the downstream end of the canal following the rapid gate closure. The water piled up against the closed gate leading to the wave formation and its upstream translation. Initially the compression wave shape evolved with time in response to the asymmetrical channel shape and the rapid change in wetted area and shape during the wave generation and initial acceleration. Further upstream, i.e. x < 14 m, the shape of the compression wave evolved more gradually, and became nearly unchanged at the observation point x = 8.6 m. There, the free-surface elevation rose very rapidly during the wave passage. Instantaneous free-surface elevation and velocity measurements were recorded synchronously at relatively high frequency (100 and 200 Hz). Figure 5 shows typical data sets for a breaking surge with undulations, in terms of the water surface elevation z and longitudinal velocity component V_x, positive downstream, at different transverse locations y. In Figure 5, the data are ensemble-averaged and z is the free-surface elevation above the lowest bed elevation. The curves include the ensemble-median data and, in Figure 5a, the differences between third and first quartile. The latter may be considered as a proxy of the instantaneous fluctuation.

The free-surface data showed that the surge was three-dimensional (Fig. 4 & 5b). That is, it was breaking in the shallow water side and undular in the deep-water side. Prior to the compression wave passage, the current velocity was positive downstream at all transverse elevations. The wave propagation had a marked effect on the velocity field, as seen in Figures 5a and 5b. Key features encompassed a brutal flow deceleration as well as fast fluctuations of each velocity component during and behind the compression wave front. The present observations were consistent with earlier observations in rectangular channels (Koch and Chanson 2009, Leng and Chanson 2016), albeit a key feature was the three-dimensional nature of the surge front.

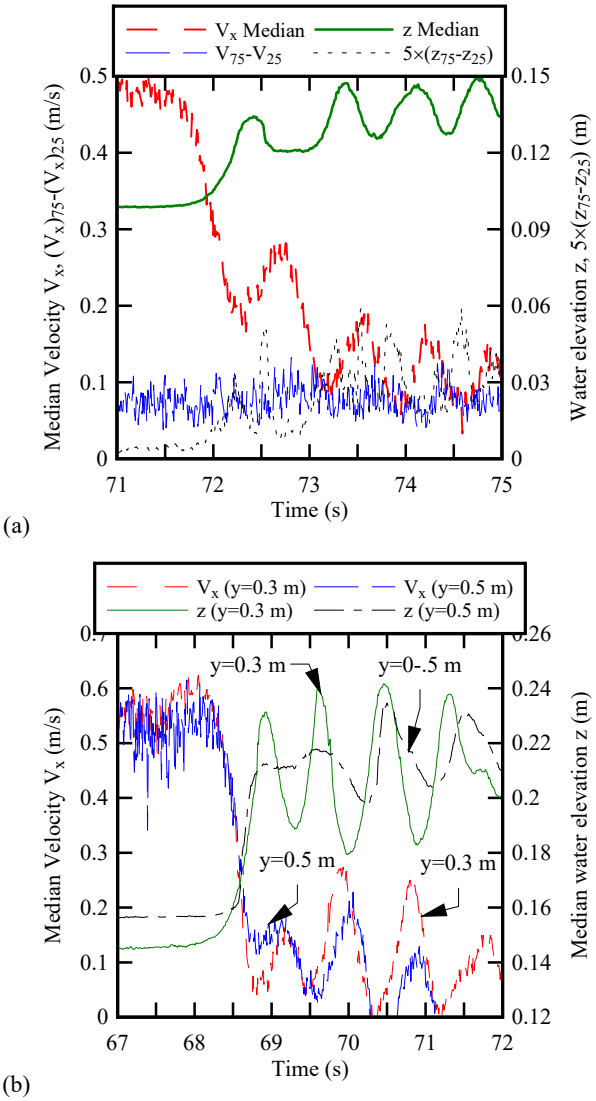

Figure 5. Time-variations of ensemble-median longitudinal velocity V_x and water surface elevation. (a) Fr_1 = 1.41, d_1 = 0.106 m, Re_1 = 0.95×10^5 at x = 8.6 m, y = 0.28 m, z_{ADV} = 0.055 m. (b) Fr_1 = 1.47, d_1 = 0.151 m, Re_1 = 1.7×10^5 at x = 8.6 m, y = 0.3 m & 0.5 m, z_{ADV} = 0.1125 m.

Conclusion

A physical investigation of compression wave was undertaken in an asymmetrical trapezoidal canal of relatively large dimensions, i.e. 19 m long and 0.7 m wide. Free-surface and velocity measurements were recorded at a relatively high frequency for a range of unsteady flow conditions. The present study was focused on the unsteady turbulent properties. The properties of the compression wave were functions of relative initial flow depth d_1/D and Froude number Fr_1. Visual and free-surface observations showed markedly three-dimensional water surface features. The compression wave was typically

undular in the deep section and breaking in the shallow section. The velocity data demonstrated a drastic impact of the compression wave on the turbulent flow field. The surge propagation induced a brutal deceleration and rapid fluctuations of all velocity components behind the front. Although the present results showed similarities to earlier observations in rectangular channels, a key difference was the three-dimensional nature of the compression wave. The findings may be directly relevant to compression wave propagation in man-made trapezoidal waterways, including hydropower canals.

Acknowledgments

The authors thank Ms Urvisha Kiri for helpful advice, and Mr Jason Van Der Gevel and Stewart Matthews for technical assistance.

References

[1] Benet, F., and Cunge, J.A. (1971). Analysis of Experiments on Secondary Undulations caused by Surge Waves in Trapezoidal Channels. *Journal of Hydraulic Research*, IAHR, Vol. 9, No. 1, pp. 11-33.

[2] Berry, M.V. (2018). Minimal analytical model for undular tidal bore profile; quantum and Hawking effect analogies. *New Journal of Physics*, Vol. 20, 053066, 11 pages (DOI: 10.1088/1367-2630/aac28).

[3] Cabonce, J., Fernando, R., Wang, H., and Chanson, H. (2018). Using Small Triangular Baffles to Facilitate Upstream Fish Passage in Standard Box Culverts. *Environmental Fluid Mechanics*, (DOI: 10.1007/s10652-018-9604-x) (In print).

[4] Chanson, H. (2004). *Environmental Hydraulics of Open Channel Flows*. Elsevier-Butterworth-Heinemann, Oxford, UK, 483 pages.

[5] Chanson, H., Reungoat, D., Simon, B., and Lubin, P. (2011). High-Frequency Turbulence and Suspended Sediment Concentration Measurements in the Garonne River Tidal Bore. *Estuarine Coastal and Shelf Science*, Vol. 95, No. 2-3, pp. 298-306 (DOI 10.1016/j.ecss.2011.09.012).

[6] Cunge, J.A, (1966). Comparaison des Résultats des Essais d'Intumescences Effectués sur le Modèle Réduit et sur le Modèle Mathématique du Canal Oraison-Manosque. *Journal La Houille Blanche*, No. 1, pp. 55-69 & 79 (In French).

[7] Foglizzo, T., Kazeroni, R., Guilet, J., Masset, F., Gonzalez, M., Krueger, B.K., Novak, J., Oertel, M., Margueron, J., Faure, J., Martin, N., Blottiau, P., Peres, B. and Durand, G. (2015). The Explosion Mechanism of Core-Collapse Supernovae: Progress in Supernova Theory and Experiments. *Publications of the Astronomical Society of Australia (PASA)*, Vol. 32, e009, 17 pages (DOI: 10.1017/pasa.2015.9).

[8] Henderson, F.M. (1966). *Open Channel Flow*. MacMillan Company, New York, USA.

[9] Jaeger, C. (1956). *Engineering Fluid Mechanics*. Blackie & Son, Glasgow, UK, 529 pages.

[10] Keevil, C.E., Chanson, H., and Reungoat, D. (2015). Fluid Flow and Sediment Entrainment in the Garonne River Bore and Tidal Bore Collision. *Earth Surface Processes and Landforms*, Vol. 40, No. 12, pp. 1574-1586 (DOI: 10.1002/esp.3735).

[11] Kiri, U., Leng, X., and Chanson, H. (2018). Positive Surge Propagation in a Non-Rectangular Asymmetrical Channel. *Hydraulic Model Report No. CH110/18*, School of Civil Engineering, The University of Queensland, Brisbane, Australia, 159 pages and 2 digital appendices incl. 5 movies.

[12] Leng, X., and Chanson, H. (2016). Coupling between Free-surface Fluctuations, Velocity Fluctuations and Turbulent Reynolds Stresses during the Upstream Propagation of Positive Surges, Bores and Compression Waves. *Environmental Fluid Mechanics*, Vol. 16, No. 4, pp. 695-719 & digital appendix (DOI: 10.1007/s10652-015-9438-8).

[13] Leng, X., and Chanson, H. (2017). Integral Turbulent Scales in Unsteady Rapidly Varied Open Channel Flows. *Experimental Thermal and Fluid Science*, Vol. 81, pp. 382–395 (DOI: 10.1016/j.expthermflusci.2016.09.017).

[14] Pan, D.Z., and Chanson, H. (2015). Physical Modelling of Tidal Bore Dyke Overtopping: Implication on Individuals' Safety. *Proc. 36th IAHR World Congress*, The Hague, The Netherlands, 27 June-3 July, Theme 4, pp. 3824-3831

[15] Ponsy, J., and Carbonnell, M. (1966). Etude Photogrammétrique d'Intumescences dans le Canal de l'Usine d'Oraison (Basses-Alpes). *Jl Soc. Française de Photogram.*, Vol. 22, pp. 18-28 (in French).

[16] Preissmann, A., and Cunge, J.A. (1967). Low-Amplitude Undulating Hydraulic Jump In Trapezoidal Canals. *Journal of Hydraulic Research*, IAHR, Vol. 5, No. 4, pp. 263-279.

[17] Reungoat, D., Leng, X., and Chanson, H. (2017). Successive impact of tidal bores on sedimentary processes: Arcins channel, Garonne River. *Estuarine Coastal and Shelf Science*, Vol. 188, pp. 163-173 (DOI: 10.1016/j.ecss.2017.02.025).

[18] Sandover, J.A., and Taylor, C. (1962). Cnoidal waves and bores. *Journal La Houille Blanche*, No. 3, Sept., pp. 443-445.

[19] Stoker, J.J. (1957). *Water Waves. The mathematical Theory with Applications*. Interscience Publishers, New York, USA, 567 pages.

[20] Treske, A. (1994). Undular Bores (Favre-Waves) in Open Channels - Experimental Studies. *Journal of Hydraulic Research*, IAHR, Vol. 32, No. 3, pp. 355-370. Discussion: Vol. 33, No. 3, pp. 274-278.

YouTube video movies

Such a bore - {http://www.afms.org.au/vid/gallery-vid005.html}

Tidal Bore Research at the University of Queensland - {https://youtu.be/q1ieo7fQ6X8}